Design, Fabrication, and Analysis of Photodynamic Therapy Oxygen Monitoring System For Use In Esophageal Carcinoma

Gemunu Happawana[1], Amaranath Premasiri[2], Arye Rosen[3]

[1]Department of Mechanical Engineering, California State University, Fresno, CA 93740, email:ghappawana@csufresno.edu, 559-278-6832, Fax: 559-278-2368.
[2]Department of Mechanical Engineering, Southern Methodist University, Dallas, TX, 75275, email:apremasi@smu.edu, 214-768-1966, Fax: 214-768-1473.
[3]Electrical and Biomedical Engineering, Bossone 7-504, Drexel University, Philadelphia, PA, 19104, email: ar86@drexel.edu, 215-895-1913, Fax: 215-895-4983

Abstract

Photodynamic therapy (PDT) is an effective and minimally invasive treatment modality with relatively fewer side effects than chemotherapy and radiation, which has been approved by the FDA for treatment of esophageal cancer. Maximum therapeutic outcome of the PDT protocol for each individual patient requires optimization of the components of PDT operating at their highest efficacy. Tumor necrosis, the method of malignant tissue destruction by PDT, is carried out by the toxic singlet oxygen molecules that are being formed from the molecular oxygen in the tumor. The availability of molecular oxygen, being the rate limiting step for PDT, plays a key role in the treatment protocol. Currently, the PDT of esophageal carcinoma is a relatively blind process since there is no method to monitor the tumor oxygen level during the treatment. In this paper, we present an optical technique to monitor molecular oxygen level in the PDT milieu. The method described herein is a reflection oximetry technique designed with small semiconductor lasers and a silicon photodiode. The light used for monitoring system comes from two semiconductor diode lasers of 650 nm and 940 nm wavelengths. The two lasers and the photodiode are integrated into a small package which is then mounted onto a balloon catheter containing the PDT light delivery system. The lasers and photodiode are powered and controlled by a control box that is connected via a cable. The light sources and the photodiode output are controlled by LabVIEW virtual instrumentation. The sequential on and off light sources and the respective reflective signals are processed with MATLAB. The latter code integrates with LabVIEW to make an automatic calculation of the corresponding light absorption by each chromophore to determine the change in oxygen level as well as the amount of blood and oxygen present in the treatment area. The designed system is capable of monitoring the change in oxygen level and the blood flow in any part of the human body where it is possible to place the package.

Key words: Photodynamic therapy, esophageal carcinoma, oxygen detection, photonic reflective oximeter

1. Introduction

Oxygen is a key element in PDT and would deplete with time[1]. Oxygen and photosensitizer level monitoring during PDT are effective ways of maintaining the optimum concentrations of this rate limiting substance throughout the treatment process. The photo bleaching of photosensitizer is also considerable during PDT. Preferably, such information should be available to clinicians on a continuous basis rather than at the beginning and at the end of the treatment. This requirement can be met non-invasively with the technology of optical detection. The optical techniques are now well established and are in regular clinical use during anesthesia and intensive care when monitoring patient vitals.

An oximeter is a commonly used biomedical instrument to detect the oxygen content in capillaries[2, 3-11]. Pulse oximeters are commonly used instruments for *in-vivo* reading[12, 13-14]. While this is not a perfect method to read the true arterial oxygen saturation of human tissues, its principle can be used to measure the relative oxygen concentration in a tumor during PDT[15]. The physics behind this technique is based on the light absorption of the two different types of hemoglobin, oxyhemoglobin (Hbo_2) and deoxyhemoglobin (Hb), in the blood stream. This work discusses the integration of an optical detection system into the PDT balloon catheter using an integrated system of detector and lasers to monitor the oxygen level and the photosensitizer concentration. Light transmitted through a tissue is detected and the portion of absorbed energy is calculated to analyze the oxygen content. Light transmitted through a chromophore is given by the Beer-Lambert equation[13].

The change in blood chromophores in the tissue can be modeled with the modified Beer-Lambert law. When the light source and the detector are located on a tissue the detector receives backscattered light. The amplitude of the light that the detector receives can be very much less, compared to the light emitted by the source, due to scattering and absorption by the tissue. Therefore, usage of high power light sources and efficient detectors to measure the backscattered light are very important in a detection system.

2. Theory of reflectance optical detection system

The physical requirement necessary for an optical system in order to detect multiple numbers of chromopores is to have light sources of specific wavelength with different absoptivity pattern. The light attenuation between the source and the detector can be written as follows:

$$-\log_{10}\left(\frac{I_{out}}{I_{in}}\right) = OD_{\lambda} \tag{1}$$

where I_{in} is the incident light, I_{out} is the detected light, and OD_{λ} is the optical density for wavelength λ. Optical density is a function of absorption (A_{λ}) and scattering (S_{λ}) of wavelength λ. Therefore, Eq.(2) can be rewritten as follows:

$$-\log_{10}\left(\frac{I_{out}}{I_{in}}\right) = OD_{\lambda} = attenuation = A_{\lambda} + S_{\lambda} \tag{2}$$

HbO_2, Hb, and the photosensitizer (PS) are the main absorber chromophores in the PDT environment. Therefore, the light absorption can be written as follows:

$$A_{\lambda} = \varepsilon_{HbO_2,\lambda} C_{HbO_2} L_{\lambda} + \varepsilon_{Hb,\lambda} C_{Hb} L_{\lambda} + \varepsilon_{PS,\lambda} C_{PS} L_{\lambda} \tag{3}$$

where $\varepsilon_{HbO_2,\lambda}$, $\varepsilon_{Hb,\lambda}$, and $\varepsilon_{PS,\lambda}$ are the specific extinction coefficient of oxyhemoglobin, deoxyhemoglobin and photosensitizing agent for wavelength λ. C_{HbO_2}, C_{Hb}, and C_{PS} are the concentrations of the oxyhemoglobin (Hbo_2), deoxyhemoglobin (Hb) and photosensitizing agent respectively, and L_λ is the optical path length. This optical path length can be expressed as source detector separation,

$$L_\lambda = d.DPF_\lambda \tag{4}$$

where d is the separation between the light source and the detector and DPF_λ is the differential path length factor. The correction for the mean photon path length for scattering, is termed the differential pathlength factor, and expressed as follows[16]:

$$DPF_\lambda = \frac{1}{2}\left(\frac{3\mu_{s,\lambda}^{/}}{\mu_{a,\lambda}}\right)^{1/2}\left[1-\frac{1}{1+d.(3\mu_{s,\lambda}^{/}\mu_{a,\lambda})^{1/2}}\right] \tag{5}$$

where $\mu_{a,\lambda}$ is the absorption coefficient and $\mu_{s,\lambda}$ is the reduced scattering coefficient at wavelength λ. Consumption of oxygen in blood, during the PDT reaction, leads to reduction in oxyhemoglobin concentration. Therefore the optical density OD_λ, varies with time. This differential OD_λ value can be written as follows:

$$\Delta OD_\lambda = OD_{\lambda,final} - OD_{\lambda,initial} = d.DPF_\lambda(\varepsilon_{HbO,\lambda}\Delta C_{HbO_2} + \varepsilon_{Hb,\lambda}\Delta C_{Hb} + \varepsilon_{PS,\lambda}\Delta C_{PS}) \tag{6}$$

Thereafter the effect of scattering is not influential to the model. Each chromophore has a specific extinction coefficient and a differential pathlength factor. Therefore, measurements with the three wavelengths give

$$\Delta OD_{\lambda_1} = d.DPF_{\lambda_1}(\varepsilon_{HbO_2,\lambda_1}\Delta C_{HbO_2} + \varepsilon_{Hb,\lambda_1}\Delta C_{Hb} + \varepsilon_{PS,\lambda_1}\Delta C_{PS}) \tag{7}$$

$$\Delta OD_{\lambda_2} = d.DPF_{\lambda_2}(\varepsilon_{HbO_2,\lambda_2}\Delta C_{HbO_2} + \varepsilon_{Hb,\lambda_2}\Delta C_{Hb} + \varepsilon_{PS,\lambda_2}\Delta C_{PS}) \tag{8}$$

$$\Delta OD_{\lambda_3} = d.DPF_{\lambda_3}(\varepsilon_{HbO_2,\lambda_3}\Delta C_{HbO_2} + \varepsilon_{Hb,\lambda_3}\Delta C_{Hb} + \varepsilon_{PS,\lambda_3}\Delta C_{PS})$$

Solving Eq.(7), Eq.(8) and Eq.(9) we obtain the general equations for three different

chromophores in blood, ΔC_{HbO_2}, ΔC_{Hb}, and ΔC_{PS}:

$$\Delta C_{HbO_2} = \frac{\Delta OD_{\lambda_3}.DPF_{\lambda_1}.DPF_{\lambda_2}.(\varepsilon_{PS,\lambda_1}.\varepsilon_{Hb,\lambda_2} - \varepsilon_{Hb,\lambda_1}.\varepsilon_{PS,\lambda_2})}{a_1} +$$

$$\frac{\Delta OD_{\lambda_2}.DPF_{\lambda_1}.DPF_{\lambda_3}.(\varepsilon_{Hb,\lambda_1}.\varepsilon_{PS,\lambda_3} - \varepsilon_{PS,\lambda_3}.\varepsilon_{Hb,\lambda_2})}{a_1} +$$

$$\frac{\Delta OD_{\lambda_1}.DPF_{\lambda_2}.DPF_{\lambda_3}.(\varepsilon_{PS,\lambda_2}.\varepsilon_{Hb,\lambda_3} - \varepsilon_{Hb,\lambda_2}.\varepsilon_{PS,\lambda_3})}{a_1} \tag{10}$$

$$\Delta C_{Hb} = \frac{\Delta OD_{\lambda_3}.DPF_{\lambda_1}.DPF_{\lambda_2}.(\varepsilon_{HbO_2,\lambda_1}.\varepsilon_{PS,\lambda_2} - \varepsilon_{PS,\lambda_1}.\varepsilon_{HbO_2,\lambda_2})}{a_1} + \frac{\Delta OD_{\lambda_2}.DPF_{\lambda_1}.DPF_{\lambda_3}.(\varepsilon_{PS,\lambda_1}.\varepsilon_{HbO_2,\lambda_3} - \varepsilon_{HbO_2,\lambda_1}.\varepsilon_{PS,\lambda_3})}{a_1} + \frac{\Delta OD_{\lambda_1}.DPF_{\lambda_2}.DPF_{\lambda_3}.(\varepsilon_{Hb,\lambda_2}.\varepsilon_{PS,\lambda_3} - \varepsilon_{PS,\lambda_2}.\varepsilon_{HbO_2,\lambda_3})}{a_1} \quad (11)$$

$$\Delta C_{PS} = \frac{\Delta OD_{\lambda_3}.DPF_{\lambda_1}.DPF_{\lambda_2}.(\varepsilon_{HbO_2,\lambda_1}.\varepsilon_{Hb,\lambda_2} - \varepsilon_{Hb,\lambda_1}.\varepsilon_{HbO_2,\lambda_2})}{a_1} + \frac{\Delta OD_{\lambda_2}.DPF_{\lambda_1}.DPF_{\lambda_3}.(\varepsilon_{Hb,\lambda_1}.\varepsilon_{HbO_2,\lambda_3} - \varepsilon_{HbO_2,\lambda_1}.\varepsilon_{Hb,\lambda_3})}{a_1} + \frac{\Delta OD_{\lambda_1}.DPF_{\lambda_2}.DPF_{\lambda_3}.(\varepsilon_{HbO_2,\lambda_2}.\varepsilon_{PS,\lambda_3} - \varepsilon_{Hb,\lambda_2}.\varepsilon_{HbO_2,\lambda_3})}{a_1} \quad (12)$$

where

$$a_1 = DPF_{\lambda_1}DPF_{\lambda_2}DPF_{\lambda_4}.d(\varepsilon_{PS,\lambda_1}\varepsilon_{Hb,\lambda_2}\varepsilon_{HbO_2,\lambda_3} + \varepsilon_{HbO_2,\lambda_1}\varepsilon_{PS,\lambda_2}\varepsilon_{Hb,\lambda_3} + \varepsilon_{Hb,\lambda_1}\varepsilon_{Hb,\lambda_2}\varepsilon_{PS,\lambda_3} - \varepsilon_{Hb,\lambda_1}\varepsilon_{PS,\lambda_2}\varepsilon_{HbO_2,\lambda_3} - \varepsilon_{PS,\lambda_1}\varepsilon_{HbO_2,\lambda_2}\varepsilon_{Hb,\lambda_3} - \varepsilon_{HbO_2,\lambda_1}\varepsilon_{Hb,\lambda_2}\varepsilon_{PS,\lambda_3})$$

The change in oxygen level and photosensitizer level is given as follows:

$$\Delta OXY = OXY_{t_1} - OXY_{t_2} \quad (13)$$

$$\Delta PS = PS_{t_1} - PS_{t_2} \quad (14)$$

where OXY and BV are oxyhemoglobin and blood volume changes:

$$OXY = \Delta C_{HbO_2} - \Delta C_{Hb} \quad (15)$$

and

$$BV = \Delta C_{HbO_2} + \Delta C_{Hb} \quad (16)$$

Therefore, a system with two different light sources and a light detector can evaluate the intensity of the incident light and the detected reflected light and thereby calculate the concentration of hemoglobin and oxyhemoglobin.

3. The system design

As explained previously there should be at least three different wavelengths to monitor the blood chromophore level and the photosensitizing agents. Many number of light sources from each wavelength, and many number of detectors can be used for this purpose. However increasing the number of devices complicates the probe geometry. The proposed detection system design consists of three semiconductor lasers for the excitation of the chromospheres and a detector. In

the device fabrication we include two light sources and a photodetector packaged together as shown in Fig.1.

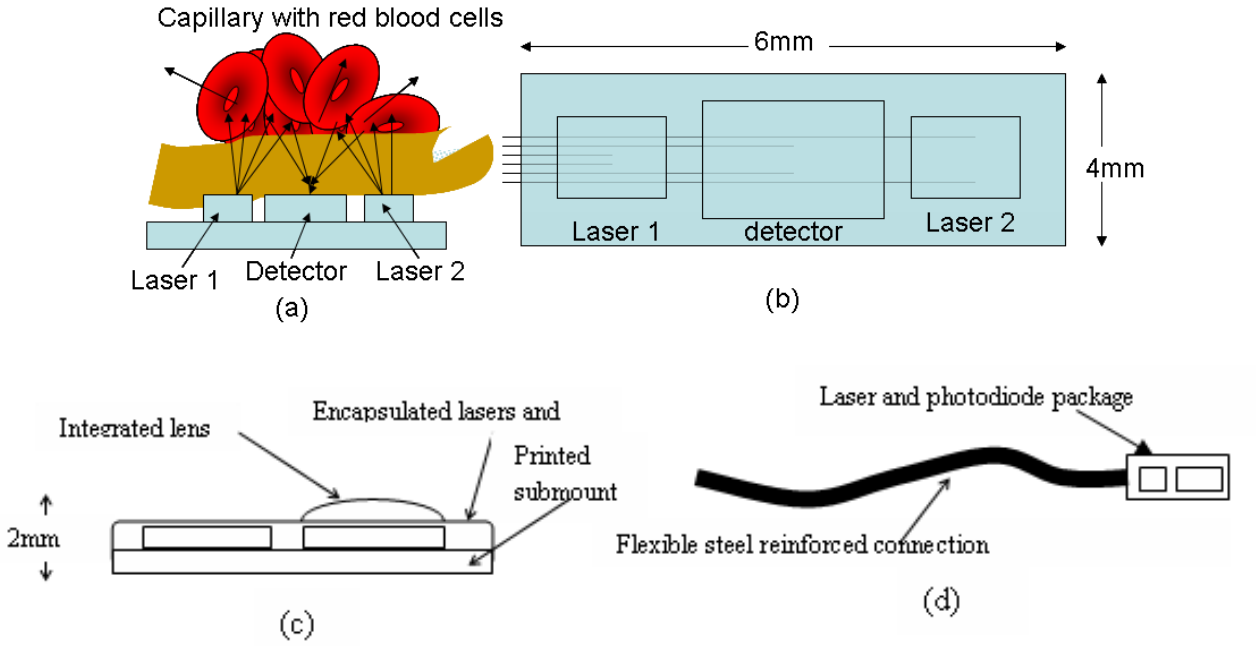

Fig.1: (a) Oxygen detection system in the presence of blood chromophore; (b) circuit for lasers and the detector; (c) encapsulated cross section with lens; and (d) system design to insert into the balloon catheter.

The prototype development and the testing could be performed with any type of photosensitizing agent. The locations of the light sources are determined by the light scattering distance of living tissue. In this work, a center-to-center distance of a light source and the detector is kept at 1cm. This distance provides sufficient spacing for the prototype fabrication and also for the detector to receive enough photons to give an appropriate signal output. The power supply, control system, and data acquisition system are connected to the insertable package. Figure 1 shows a diagram of the insertable part of the detection system.

The ideal probe to be used for PDT of esophageal carcinoma will have the following special features. The lasers and the photodetector are packaged onto a printed circuit sub-mount for miniaturization. The package is then encapsulated in a perfectly amorphous polymer to prevent the circuitry from damage during operation (Fig.1(c)). A concave lens is integrated onto the photodiode to collect maximum reflected light, as shown in Fig.1(c). The packaged lasers and the photodetector are connected to a flexible steel cable (Fig.1(d)), so that the entire detection unit can be moved inside the balloon catheter to the precise location of the tumor. Figure 2 gives a block diagram of the oxygen detection system. The oxygen detection system would be calibrated and validated using a commercially available oxygen detection system. This system is designed without an advanced laser driver; it uses a less expensive DC power supply or a 12V battery. The selection of the power supply is based on the power requirement of the semiconductor lasers and the detector bias voltage.

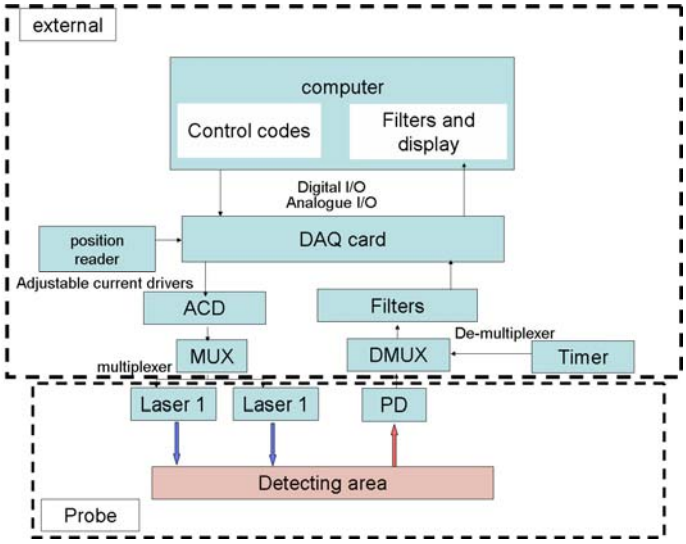

Fig.2: Schematic of the oxygen detection system.

3.1 Selection of the exciting light wavelength

Certain wavelengths transmitted, through a photosensitizing agent accumulated tissue, is absorbed by the photosensitizing agent and the agent will fluoresce upon onset of a light. The fluorescence intensity is dependent on the amount of oxygen in a tumor. A normal tissue has more oxy-hemoglobin and hence more oxygen. Fluorescence spectrum of the photosensitizing agent (Photofrin) accumulated tumor and normal tissue is shown in Fig.3. The fluorescence spectrum clearly shows the fluorescence intensity difference in the tumor and the normal tissue at a range of wavelengths. Also, as seen in Fig.3, at certain wavelengths, higher than 750 nm wavelengths, there is no difference in fluorescence spectrum by the photosensitizing agent of the tumor and the normal tissue.

The largest difference between the tumor and the normal tissue fluorescence for the Photofrin photosensitizer lies between 650nm to 675nm (Region1 in Fig. 3). The wavelengths on or above 750 nm, infrared (IR) Region 2 in Fig. 3, shows no difference in the fluorescence spectrum of the tumor and the normal tissue. Therefore, in the selection of the wavelengths the first laser is selected with 650nm and the other with 904 nm. These two selections provide a better spectral heterogeneity for the oxygen detection. Semiconductor lasers of these wavelengths are commercially available at reasonable prices.
The typical operating voltage of the 650nm semiconductor laser selected for the application is 2.3V and the maximum voltage is 2.6V. The recommended operating voltage for 904nm laser is 1.8V to 2.5V, and the suggested typical voltage is 2.0V. The operating temperature range of the 650nm laser is -10 to 70^{o}C and for the 904nm laser is -10 to +50^{o}C. These operating temperatures are adequate to drive the lasers in a low duty cycle without degrading the lasers.

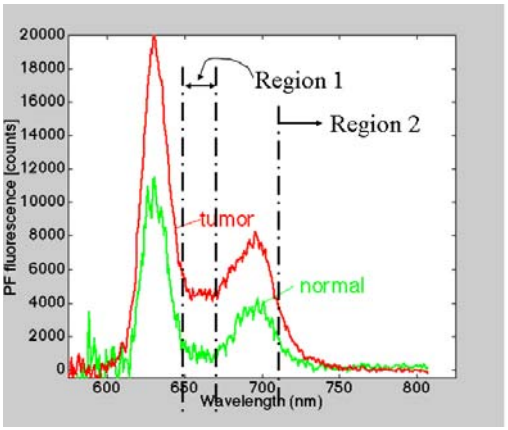

Fig. 3: Sum of the auto fluorescence and fluorescence of Photofrin in an epithelial cell[12].

3.2 Detector selection

The light detector is selected to sense the backscattered light of 650nm and 940nm. A commercially available silicon photodiode with a spectral response of 350-1100 nm is used for the package to detect the range of light (including detection of the fluorescence of a photosensitizer). The rise and fall times of the photodiode are both 10ns at 20V bias voltage with a 50Ω load. This is, therefore, well suited for this application since the current saturation does not interfere with the light emitting sequence. The active area of this detector is 13mm^2 and the detector is packaged in a standard T05 (0.36") submount. This packaged detector is used only for the prototype deign. In an actual device fabrication, the detector and the lasers could be imprinted onto a balloon catheter for smaller size devices.

4. Control system layout and oxygen monitoring technique

The two lasers in the probe are driven by a simple DC power supply. Duty cycles of the lasers are determined by the detector rise time, fall time and also the operating temperatures of the lasers. Both selected lasers show high operating temperatures, although it is preferable to keep the laser operating temperature at a stable point to avoid wavelength shift. Therefore the laser controlling circuit is designed with a timing component that makes the laser drive in for a very short time period, which is necessary to excite the monitoring area. A National semiconductor TLC555 timer is used as the center component of the timing circuit. The timer capacitance and the resistors are used in such a way that the current is driven in the circuit within one tenth of a second.

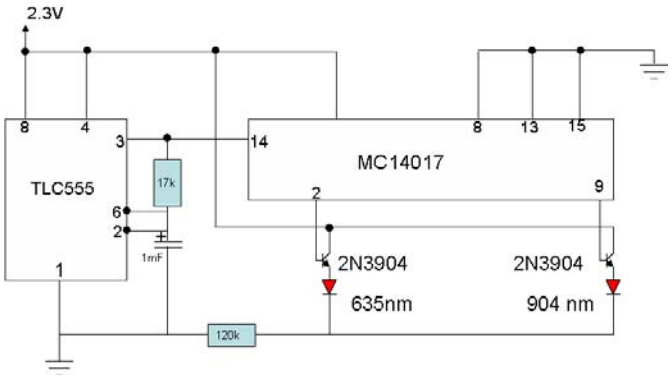

Fig.4: Laser controlling circuit with 2.3V power input

The timer output current is divided into separate two channels, using a decade counter as shown in the Fig.4. MC14017B five-stage Johnson decade counter is used in the circuit. This consumes very little power and gives a spike-free output. The decade counter can supply ten separate leads. In this application, only two leads are used while the rest are kept grounded. The circuit is set up to operate on each laser in a pulsed mode with every 0.9 second pulsed width and 0.05 second dwell to avoid thermal buildup inside the lasers. The lasers are connected to the emitter of an NPN transistor, whose base is connected to the main power supply, and the collector to the decade counter output. In this way, the laser power input is kept constant and at an expected value. The lasers are connected to the decade counter through transistors, where the main power source to lasers is connected. The silicon detector is connected to a 12V bias voltage supply. This is the supply voltage to the controlling circuit. The laser driving voltage of 2.3V is supplied from this source, through a voltage divider.

5. Fabrication of blood oxygen monitoring system

5.1 Probe design

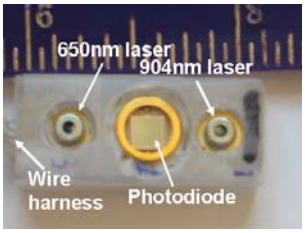

Fig. 5: Prototype of the probe design

For the prototype fabrication we have used packaged lasers and a germanium photodiode due to commercial availability and cost effectiveness. Un-packaged devices can be easily incorporated into the probe when the prototype design is verified with the experimental data. In the final design, the probe was encapsulated with a transparent polymer material to protect the complete circuitry from shear forces generated during insertion of the balloon catheter system into the esophagus. As shown in Fig. 5, the photodiode and lasers are packaged in a Teflon block. The wire connections for the detector and the lasers are at the bottom of the package, firmly connected to the block, where possible mishandling would not damage the wire connections.

5.2 Data acquisition and data acquisition system

LabVIEW (National Instruments) is used for data acquisition and the desired output. NI-DAQmx a subprogram in the LabVIEW is used in developing the virtual instrumentation for the oxygen detection system, which is now used in most of the industrial setting for data acquisition and instrument control.

The front panel of the LabVIEW consists of three different waveform charts that provide the raw detector signal without digital filtering, the digitally filtered input signal, and the variation of hemoglobin and oxyhemoglobin. NI 6221 DAQ card was used with SCB-68 shielded I/O connector block. The SCB-68 opens the connection to the controller circuit with virtual instrumentation. The detector voltage outputs that belong to the respective lasers are fed to the connector block. LabVIEW DAQ, signal conditioning hardware and software, provides graphical development of the control. DAQmx detector output signal is split into two signals as the initial step in the process. These signals are acquired with a certain time difference, which is removed by modifying the signal at second stage by adding the time difference to the trailing signal. Optical input to output ratio is calculated thereafter. The signal is then sent through a band pass filter before it is input to the mathscript node.

6. The experimental setup

The experimental setup consists of the proto board where the controlling circuit was built, two power supplies, two multimeters and a personal computer in which NI LabVIEW was installed. The detector reading acquired by the LabVIEW program is validated with the multimeters connected to the physical channel of the detector output. The circuit design is assumed to have zero generation of crosstalk, since the current and signals always travel in one path at any given time. Following this, the interference of signals in different paths is minimal and the noise generated is negligible.

The actual system does not consist of these additional equipments. Final instrumentation consists only of the DC power supply, in addition to the controlling circuit and the probe. The DC power supply is set for the 12V output, which is necessary for the detector reverse voltage. This system can be easily powered by a 12V battery pack, when there is no main power supply available. The preliminary testing with the probe and the detection system was done with the upper limb of the author. Even though the system is designed for the use in esophagus, it is not possible to conduct an in-vivo testing with the esophageal tissue under currently available laboratory conditions. The probe was moved to several places to observe uninterrupted reading, yet it was noted that the pulsative blood flow adds a degree of noise to the reading. This noise however, does not to the general reading required to monitor the oxygen level.

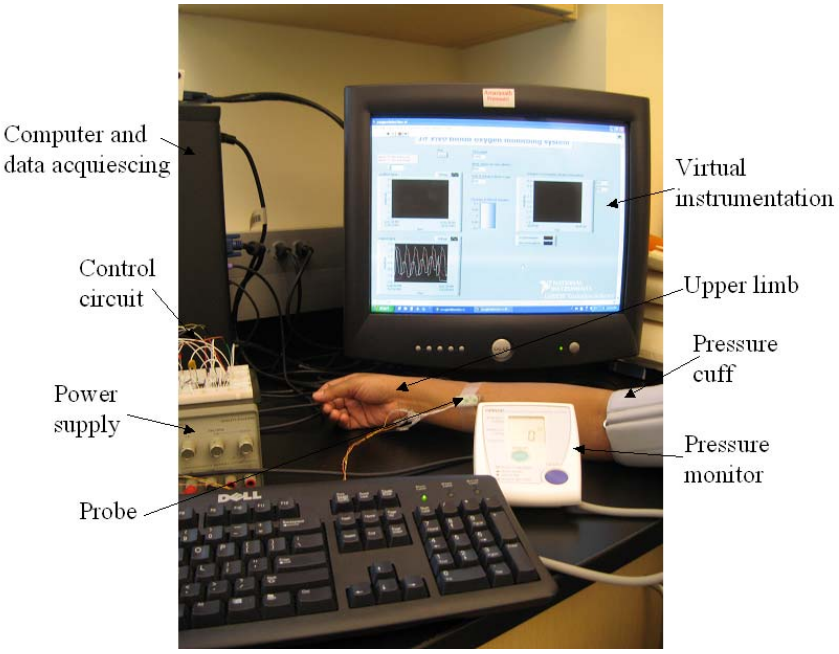

Fig.6: Testing of the oxygen detection system on human upper limb to evaluate the detector capability. The experiment is conducted to see the signal capturing of the diode detector.

6. Preliminary results

A set of experimental results was obtained to validate the probe design and the data acquisition system, using the author's upper arm. The probe was firmly held against the skin by a tape, as shown in Fig.6. The absorption and scattering of 904 nm light is comparatively less than that of 650nm light. Therefore the ratio of the light signal emitted by the laser to the light signal received by the detector is higher in the higher wavelengths. The detector signal was slightly different when the probe was placed on the limb since the blood flow, in pulsatile manner, adds noise to the detector signal. This noise does not deteriorate the monitoring process since it was present throughout. Attenuation is possible by selecting a monitoring location such as the ear lobe, with minimal interruption by other blood vessels. However, the selection of such a placement is only necessary for calibration purpose, since the final probe design should be able to monitor the esophageal environment, which is closer to the heart.

The final set of reading was obtained to verify the system capability to capture a change in blood oxygen level. Application of a 140 mmHg pressure to upper limb, which is above the systolic blood pressure for a particular subject, will cut off the blood supply completely for the period of pressure application. As a consequence, the fraction of deoxyhemoglobin in the distal part of the upper limb is increased. The difference of oxyhemoglobin and deoxyhemoglobin is detected by the monitoring system, as shown by the separation of the two data lines (Fig.7). Figure 7 illustrate the oxyhemoglobin (—◆—) reading and deoxyhemoglobin (—■—) reading for 120 second where application of pressure is initiated in 20 second after the beginning of the reading. Further verification of the system with Photofrin® contacting environment is required to test how far the system fulfills the design objective

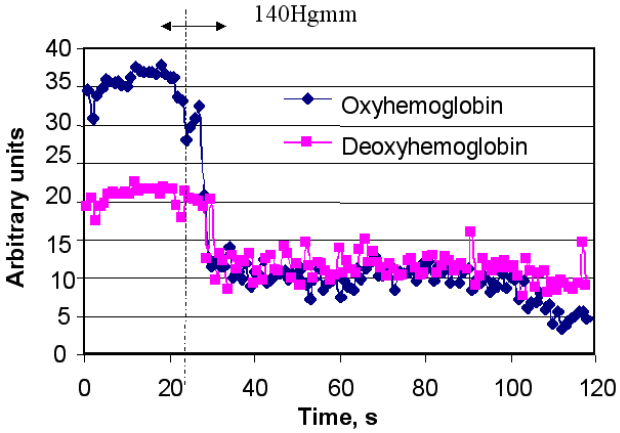

Fig.7: oxyhemoglobin and deoxyhemoglobin readings when 140Hgmm pressure is applied.

7. Discussion

A photonic reflectance oximeter is designed, analyzed, and fabricated. The specific device selection, to be used alone with PDT, is discussed. The application of the designed system is not specific to esophagus. The system is designed either to be used inside an internal organ or on the skin, where melanin plays a major role in light scattering and absorption. The virtual instrumentation is developed to change its formulation in accordance with the location of the monitoring. The virtual instrumentation instantly gives the change in blood oxygen content and the blood volume. The absolute change in oxygen level can be derived by calibrating the system, using existing oxygen monitoring systems. The change of oxyhemoglobin and deoxyhemoglobin is given relative to the initial level of each component. This is am important advancement in the case of PDT.

The prototype used commercially available lasers and detectors so that the current probe is relatively large in size to be compared to the light delivery system to be designed for the esophagus. However, it is not a complicated task to fabricate a probe that can be imprinted onto a balloon catheter. The oxygen detection system can be further modified and incorporated into the light detection system, added to the rear side of the detector probe, for monitoring of the photosensitizer fluorescence signal. All commercially available photosensitizers give a significant fluorescence signal that can be easily filtered and used for monitoring purposes.

References

1. J. D. Chapman, C.C. Stobbe, M.R. Arnfield, R. Santus, J.lee, and M.S. McPhee, " Oxygen dependency of tumor cell killing in vitro by light-activated Photofrin II", Radiat. Res, Vol.126, no.1, pp.73-79, 2005.
2. D. J. Robinson, H. S. de Bruijn, d. van, V, M. R. Stringer, S. B. Brown, and W. M. Star, "Fluorescence photobleaching of ALA-induced protoporphyrin IX during photodynamic therapy of normal hairless mouse skin: the effect of light dose and irradiance and the resulting biological effect," Photochem. Photobiol., vol. 67, no.1, pp. 140-149, 1998.
3. A. Curnow, J. C. Haller, and S. G. Brown, "oxygen monitoring during 5-amonolaevulinic acid induced photodynamic therapy in normal rat colon. Comparison of continuous and fractionated light regime", J.Photochem.Photobiol.B, Vol.58, no.2-3,pp.149-155, 2000.

4. Jr. Edgar, W. Reuben, Gilstad, W. Dennis, Branstetter., and L. Ronald, "Method and apparatus for noninvasive monitoring of arterial blood oxygen saturation,"4714080, 1987.
5. R. L. Sheridan, K. M. Prelack, L. M. Petras, S. K. Szyfelbein, and R. G. Tompkins, Intraoperative reflectance oximetry in burn patients," J. Clin. Monit., vol. 11, no. 1, pp. 32-34, 1995.
6. S. Nioka, M. Izzetoglu, T. Mawn, M. J. Nijland, D. Boas, and B. Chance, "Fetal transabdominal pulse oximeter studies using a hypoxic sheep model," J. Matern. Fetal Neonatal Med., vol. 17, no. 6, pp. 393-399, 2005.
7. M. J. Decker, D. Dickensheets, J. L. Arnold, P. W. Cheung, and K. P. Strohl, "A comparison of a new reflectance oximeter with the Hewlett-Packard ear oximeter," Biomed. Instrum. Technol, vol. 24, no. 2, pp. 122-126, 1990.
8. T. Durduran, G. Yu, M. G. Burnett, J. A. Detre, J. H. Greenberg, J. Wang, C.Zhou, and A. G. Yodh, "Diffuse optical measurement of blood flow, blood oxygenation, and metabolism in a human brain during sensorimotor cortex activation," Opt. Lett., vol. 29, no. 15, pp. 1766-1768, 2004.
9. J. Ling, S. Takatani, G. P. Noon, and Y. Nose, "In-vivo studies of reflectance pulse oximeter sensor," in Physiological Imaging, Spectroscopy, and Early Detection Diagnostic Methods, SPIE, 1887, pp. 256-262,1993.
10. I. Charamisinau, K. Keymel, W. Potter, and A. R. Oseroff, "Handheld dual fluorescence and reflection spectroscopy system for monitoring topical low dose ALA-PDT of actinic keratoses (AK)," Optical methods for tumor treatments and detection: mechanisms and techniques in photodynamic therapy XV, SPIE, 6139, 2006, pp. 318-327.
11. A. E. El-Desoky, A. Seifalian, M. Cope, D. Delpy, and B. Davidson, "Changes in tissue oxygenation of the porcine liver measured by near-infrared spectroscopy," Liver Transpl. Surg., vol. 5, no. 3, pp. 219-226, 1999.
12. S. Mitra and T. H. Foster, "Photochemical oxygen consumption sensitized by a Porphyrin phosphorescent probe in two systems," Biophysical Journal, vol. 78, pp. 2597-2605, 2000.
13. J. G. Webster, Design of pulse oximeters, 1 ed J. W. Arrowsmith Ltd,Bristol, UK, 1997.
14. M. Fernandez, K. Burns, B. Calhoun, S. George, B. Martin, and C. Weaver, "Evaluation of a new pulse oximeter sensor," Am. J. Crit Care, vol. 16, no. 2, pp.146-152, 2007.
15. A. Cohen and N. Wadsworth, "A light emitting diode skin reflectance oximeter," Med. Biol. Eng, vol. 10, no. 3, pp. 385-391, 1972.
16. A. Bozkurt, A. Rosen, H. Rosen, and B. Onaral, "A portable near infrared spectroscopy system for bedside monitoring of newborn brain", Biomed Eng Online, vol.4, no.29, 2005.

BIOGRAPHIES

Dr. Gemunu S. Happawana is an associate professor in the department of mechanical engineering at California State University, Fresno. Dr. Happawana holds a Ph.D. (1994) in mechanical engineering and Master of Science degree (1988) in mathematics from Purdue University, and Bachelor of Science degree (1984) with honors in mathematics from University of Colombo, Sri-Lanka. His work lies in the fields of mechanical vibration, applied mechanics and photonics, and it combines physical modeling, analytical techniques, and measurement. Dr. Happawana serves as advisor to Mini-Baja and Formula SAE student competitions. Dr. Happawana is a consultant to the high tech photonics company, Photodigm, Inc., Dallas, Texas, since 2000. He is named as Patton Industry Faculty Fellow. He has worked on converting gasoline engines to run on ethanol, natural gas or kerosene. He has more than fifty journal and conference papers, one book and two patents pending. He has graduated four Ph.D. students and served on over twenty Ph.D. and MS committees. Affiliations: SAE (member), ASME (member), OSA (member).

Dr. Amaranath Premasiri received a BSc. degree in Materials Engineering (1999) and MEng degree in Mechanical Engineering (2003) from University of Moratuwa, Sri Lanka. He served on the faculty of Mechanical and Manufacturing Engineering of the University of Ruhuna, Sri Lanka between 2000 and 2003. He earned his Ph.D. in mechanical engineering (2008) from Southern Methodist University, Dallas, Texas. He is currently serving as a senior member of the technical staff at Akon, Inc, San Jose, CA. His research area is focused on opto-electronic packaging. He has authored more than 15 peer-reviewed publications on this subject.

Dr. Arye Rosen (M'77–SM'80–F'92) received the Masters degree in engineering from Johns Hopkins University, Baltimore, MD, the M.Sc. degree in physiology from Jefferson Medical College, Philadelphia, PA, and the Ph.D. degree in electrical engineering from Drexel University, Philadelphia, PA. Dr. Rosen, has been involved in research and development of microwave/millimeter-wave devices and circuits, microwave optical interaction,

high-power semiconductor lasers and the utilization of energies for application in therapeutic medicine for the past 40 years. He also holds the title of Associate in Medicine at Jefferson Medical College, where he has been engaged in research in the Division of Cardiology since 1970. He has authored more than 200 technical papers, co-edited two books and authored six book-chapters in the field of engineering and medicine. He holds over 60 U.S. patents in the fields of engineering and medicine. Dr. Rosen is an elected Member of the National Academy of Engineering, "For contributions to microwave and laser technologies and the medical applications of these technologies." (2002). He is an Elected Member of The Franklin Institute's Committee on Science and the Arts (2003), and a Member of the John Scott Award Advisory Committee, City of Philadelphia Board of Directors of City Trusts (2004). He is a Life Fellow of IEEE, elected in 1992 "For innovation in semiconductor devices and circuits for use in microwave systems and for microwave applications to medicine." He was IEEE Distinguished Microwave Lecturer from 1997 to 2000, during which time he has presented his and the work of others in the U.S., Japan, Europe and the Middle East. He is the recipient of numerous awards, including the IEEE Third Millennium Medal (January 2000) and an IEEE Microwave Application Award (June 2000). He was also the recipient of a 1989 IEEE Region One Award and a 1997 Drexel University College of Engineering, Electrical and Computer Engineering Department, Distinguished Alumni Award.